Reports

A fluorescent GTP analog as a specific, high-precision label of microtubules

Erik K. Anderson and Douglas S. Martin
Department of Physics, Lawrence University, Appleton, WI, USA

BioTechniques 50:43-48 (July 2011) doi 10.2144/000113703
Keywords: Microtubules; fluorescence; TIRF; FIONA; cytoskeleton

Supplementary material for this article is available at www.BioTechniques.com/article/113703.

Fluorescent imaging of cytoskeletal structures permits studies of both organization within the cell and dynamic reorganization of the cytoskeleton itself. Traditional fluorescent labels of microtubules, part of the cytoskeleton, have been used to study microtubule localization, structure, and dynamics, both in vivo and in vitro. However, shortcomings of existing labels make imaging of microtubules with high precision light microscopy difficult. In this paper, we report a new fluorescent labeling technique for microtubules, which involves a GTP analog modified with a bright, organic fluorophore (TAMRA, Cy3, or Cy5). This fluorescent GTP binds to a specific site, the exchangeable site, on tubulin in solution with a dissociation constant of 1.0 ± 0.4 μM. Furthermore, the label becomes permanently incorporated into the microtubule lattice once tubulin polymerizes. We show that this label is usable as a single molecule fluorescence probe with nanometer precision and expect it to be useful for modern subdiffraction optical microscopy of microtubules and the cytoskeleton.

Fluorescence labeling is a standard tool for studies of structure and dynamics in biological systems. Recent improvements in single molecule fluorescence localization, such as stochastic optical reconstruction microscopy (STORM) (1) and photoactivated localization microscopy (PALM) (2), have permitted near electron-microscope resolution of cellular structures. Fluorescence imaging with one-nanometer accuracy (FIONA) has been used to study dynamics in motor protein and membrane systems in vivo and in vitro (3–5). A key requirement to image structures with high precision is the use of a bright organic fluorophore targeted to a specific structural position in the system of interest.

One such system is the microtubule component of the cytoskeleton. Microtubules are micrometer-long, 25-nm wide polymers of tubulin that span most animal cells. Microtubules play a role in a number of cellular functions, including intracellular transport and cell division, in conjunction with a wide variety of microtubule-associated proteins (MAPs) (6). Motor proteins combined with polar microtubules result in unidirectional transport to a well-defined destination, for example, the nerve growth cone in fast axonal transport (7). Intrinsic microtubule dynamics (8) permit rapid reconfiguration of the cytoskeleton, and MAPs associated with microtubule stabilization and destabilization, such as MAP1 and katanin, regulate these intrinsic dynamics in cells (9).

To study microtubule function in vivo and in vitro, fluorescent probes have been used to examine properties such as microtubule localization, transport, dynamics, and stiffness. Immunofluorescent labeling of microtubules in fixed cells has been used to study microtubule localization (10–12). Injection into live cells of tubulin covalently labeled with an organic fluorophore has been used to study both localization and microtubule dynamics (polymerization and depolymerization) (13–15). In vitro, covalent labeling has been used for dynamics and stiffness studies (16,17). Fluorescently modified paclitaxel, a small molecule that stabilizes microtubules against depolymerization, has been used to study microtubule localization in vivo and microtubule interactions in vitro (18,19). Green fluorescent protein-tubulin fusions have likewise been used for studies of microtubule localization and dynamics in live cells (20,21). Finally, a fluorescent GTP analog has been used to polymerize microtubules in vitro (22).

However, the existing fluorescent labels of microtubules and tubulin suffer from a number of drawbacks. Immunofluorescent labeling requires fixed cells and therefore cannot be used to investigate microtubule dynamics. Covalent labeling of tubulin with organic fluorophores is typically done at a random surface amine, which leads to uncertainty in the structural localization of the fluorophore. The drug paclitaxel inhibits microtubule depolymerization and cannot be used to study microtubule dynamics. The existing fluorescent GTP analogs either prevent polymerization (23) or are so dim as to eliminate the possibility of single fluorophore imaging, useful in both dynamics and structural studies of microtubules. In particular, there is a need for a structurally specific, permanent, bright fluorophore to label tubulin to take advantage of the capabilities of high precision optical techniques such as FIONA, STORM, and PALM. Such a high-precision label could be used to answer questions regarding long-range kinesin interactions via microtubule structure (24) or dynamic changes in microtubule protofilament number upon paclitaxel binding (25) or tau binding (26).

In this work, we present a complementary fluorescent label of microtubules that does

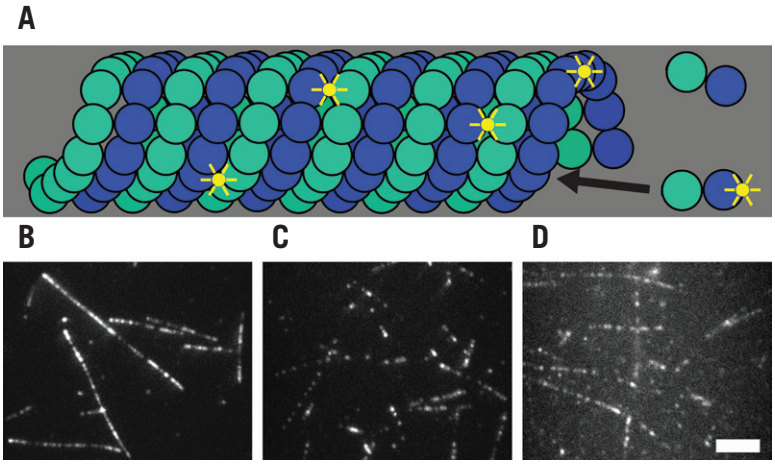

Figure 1. Microtubules labeled by fluorescent GTP analogs. (A) Cartoon showing scheme for labeling of microtubules by a fluorescent GTP analog. The tubulin dimer is represented by a green (α-tubulin) and blue (β-tubulin) circle together. The bright yellow spots represent a molecule of the fluorescent GTP analog, bound to the exchangeable GTP binding site of the tubulin dimer. Once incorporated into a microtubule, the fluorescent GTP remains bound to the E-site. (B–D) TIRF microscopy images of microtubules labeled by (B) TAMRA-EDA-GTP, (C) Cy3-EDA-GTP, and (D) Cy5-EDA-GTP, with added [fluorescent GTP]/[GTP] of 1/5. Scale bar, 5 µm.

not suffer from the above limitations. A fluorescent GTP analog, TAMRA-EDA-GTP (27), now commercially available, along with Cy3-EDA-GTP and Cy5-EDA-GTP are used to visualize microtubules in vitro. These analogs are bright enough for single molecule studies, specific to the exchangeable GTP binding site on tubulin, permanently incorporated into the microtubule lattice, and do not interfere with the binding and action of a prototypical MAP, the motor protein kinesin-1.

Materials and methods

Microtubule labeling and polymerization

Microtubules were labeled by fluorescent GTP analogs as part of the microtubule polymerization procedure from Weisenberg (28), modified as follows. Tubulin protein was purified from calf brains (29) and stored in 0.5-mg aliquots in 0.2 mM GTP at -80°C. Tubulin, GTP, and either TAMRA-EDA-GTP, Cy3-EDA-GTP, or Cy5-EDA-GTP (NU-820-TAM, NU-820-CY3, NU-820-CY5, respectively; Jena Bioscience, Jena, Germany), hereafter referred to as fluorescent GTP, were mixed with glycerol microtubule buffer (MT buffer: 80 mM PIPES, 10 mM $MgCl_2$, 1 mM EGTA, 30% v/v glycerol, pH 7.0) to typical final concentrations of 5 mg/mL tubulin, 0.1 mM to 3.2 mM GTP, and 0.02 mM fluorescent GTP (Table 1, step 3). This dilution resulted in a typical volume of 100 µL 5 mg/mL tubulin in a 1.5-mL microcentrifuge tube. Paclitaxel (Cat. no. P-9600; LC Laboratories, Woburn, MA, USA) from stock (4 mM in DMSO, stored at -80°C) was added (Table 1, step 5) to stabilize the microtubules. The microtubules were centrifuged through a room temperature sucrose cushion (50 mM imidazole, 50 mM KCl, 4 mM $MgCl_2$, 2 mM EGTA, pH 6.7, 30% w/v sucrose, 40 µM paclitaxel added just before use). Centrifugation caused polymerized microtubules to pellet through the cushion, while the remaining free tubulin and fluorescent GTP stayed above the sucrose cushion and could be removed (Table 1, steps 6–10). The pellet of microtubules was resuspended in room temperature storage buffer (50 mM imidazole, 50 mM KCl, 4 mM $MgCl_2$, 2 mM EGTA, pH 6.7, 40 µM paclitaxel added just before use), with a final concentration of approximately 5 mg/mL tubulin. The microtubules were then stored at room temperature in the dark (to prevent photobleaching) for up to 2 weeks before viewing.

Imaging

Fluorescent GTP-labeled microtubules were viewed by a custom-built total internal reflection fluorescence (TIRF) microscope (30). The fluorophore was excited using a 532-nm laser at approximately 5 mW source power (Ventus VIS 532; LaserQuantum, Stockport, UK) and imaged via a low light amplified charge-coupled device (CCD) camera (iXon DV 897; Andor Technology, Belfast, Ireland). In preparation for viewing, the solution of polymerized microtubules was diluted to between 0.25 µg/mL and 0.25 mg/mL in storage buffer to enable single microtubule viewing. This diluted microtubule solution was then washed into a flow cell made with one 24 × 60 mm, No. 1-1/2 glass coverslip (VWR, West Chester, PA, USA) treated with VECTABOND (Cat. no. SP-1800; Vector Laboratories, Burlingame, CA, USA) according to the manufacturer's instructions, and one 22 × 22 mm No. 1 glass coverslip, separated by either a thin layer of high-vacuum grease (Dow Corning, Midland, MI, USA) or double-sided tape. The VECTABOND treatment caused the microtubules to adhere to the slide surface. To reduce photobleaching of the fluorescent GTP, an oxygen-scavenging solution (5) consisting of storage buffer with 6 mg/mL glucose, 166.5 U/µL glucose oxidase (Cat. no. G2133; Sigma-Aldrich, St. Louis, MO, USA), 260 U/µL catalase (C100; Sigma-Aldrich), and 1% 2-mercaptoethanol was washed over the microtubules prior to laser illumination and viewing.

Kinesin-1–quantum dot binding to microtubules

For some experiments, a control was required to confirm the existence of microtubules that were sparsely labeled or completely unlabeled by fluorescent GTP. The existence of microtubules was tested by taking advantage of the specific binding of kinesin-1 to microtubules. Streptavidin-conjugated fluorescent quantum dots (Cat. no. Q10121MP; Invitrogen, Carlsbad, CA, USA) and biotin-kinesin (31) were diluted to 20 nM in storage buffer, mixed, and incubated for 15 min to form a kinesin-quantum dot complex. This solution was further diluted to 10 pM in the oxygen-scavenging solution with 1 mM AMP-PNP (Cat. no. A2647; Sigma-Aldrich) and washed into the flow cell. The kinesin-quantum dot complex binds to microtubules specifically and tightly in the presence of AMP-PNP. At 10 pM, kinesin-quantum dot complexes were separated by more than the diffraction limit. Labeling density was determined by counting kinesin-quantum dot complexes and dividing by microtubule contour length.

Microtubule gliding assay

To test whether kinesin-1 motility was prevented by TAMRA-EDA-GTP, a microtubule gliding assay was performed, essentially as described previously (32), with the following modifications. The biotin-kinesin (K401-BIO) used for quantum-dot binding was used, and the imaging was performed as described above.

Fluorescence labeling analysis

To identify the presence or absence of labeling, image analysis was initially done qualitatively by eye. To quantify the degree of microtubule labeling by fluorescent GTP, the following general algorithm was used. First, for a given sample, flow cell, and imaging condition, the intensity of a single fluorophore I_s was measured by integrating the image intensity of a small

region containing a single spot before and after photobleaching. Second, the intensity per unit length of a microtubule I_m was calculated by (*i*) integrating the intensity of a region containing a microtubule, (*ii*) subtracting the background that was found by integrating the intensity of an identically sized region adjacent to the microtubule, and (*iii*) dividing this background-subtracted intensity by the length of the microtubule. The number of fluorophores per unit length was calculated by dividing I_m by I_s. The fraction of exchangeable GTP sites labeled was calculated by dividing the number of fluorophores by the number of sites, based on a 13 protofilament, 8 nm tubulin dimer model of a microtubule (i.e., 1.6 sites/nm). Each of the intensity measurements was made using Solis (i) software (Andor Technology, Belfast, Ireland).

FIONA analysis

Single particle tracking of fluorescent spots was done combining the techniques of Yildiz et al. (5) and Crocker and Grier (33) in a custom program written in IDL (ITT, Boulder, CO, USA). Briefly, the particle tracking of Crocker was used to identify candidate particles; high precision positions were found using a Gaussian fit to the intensity profile as described by Yildiz et al. (5).

Microtubule depolymerization

To check whether the labeling technique allows microtubule depolymerization, microtubules were polymerized in the presence of TAMRA-EDA-GTP as described, except that paclitaxel was not added in step 5 (Table 1). After centrifugation, a microtubule pellet was still observed. Following a brief (10-min) cold incubation, polymerized microtubules were no longer observed under the microscope.

Results and discussion

Rationale

The tubulin dimer, the unit that polymerizes into a microtubule, contains exactly two GTP binding sites. The nonexchangeable (N) site at the interface of the α- and β-tubulin subunits irreversibly binds GTP prior to tubulin purification (34). The exchangeable (E) site, on the β-tubulin subunit (35), allows GTP to bind and unbind in unpolymerized tubulin, but becomes inaccessible to GTP exchange once the tubulin dimer is incorporated into a microtubule (36). As a previous study had shown that GTP modified at the 2′ or 3′ position on the ribose is incorporated into microtubules (22), we chose to test whether GTP modified at the 2′ or 3′ location with a bright, single molecule fluorescence-capable fluorophore (TAMRA, Cy3, or Cy5) would bind to the E-site of the tubulin dimer and become incorporated into microtubules (see Figure 1A). We found that microtubules polymerized in vitro in the presence of small amounts of fluorescent GTP and larger amounts of unlabeled GTP do become fluorescently labeled (Figure 1, B–D), albeit relatively sparsely (at about 1% of available sites) due to the low affinity of tubulin for fluorescent GTP (see competition assay, below).

While we anticipated E-site labeling by fluorescent GTP, microtubule labeling by fluorescent GTP could alternatively be due to nonspecific binding or binding at sites other than the E-site of tubulin. To distinguish between binding at the E-site and at another nonspecific site, we performed two types of control experiments. Since each fluorescent GTP analog labeled microtubules similarly (Figure 1, B–D), we chose to use TAMRA-EDA-GTP for further characterization. To test whether TAMRA-EDA-GTP binds nonspecifically to the surface of already polymerized tubulin, we polymerized tubulin in the presence only of unlabeled GTP to create nonfluorescent microtubules. TAMRA-EDA-GTP was then added after step 5 of the protocol in Table 1, followed by further incubation at 37°C to allow for

Power *and* Performance
at your fingertips

- Live sensor feedback for superior temperature control
- Large graphical touch screen user interface
- 96 well gradient thermal cycler
- Rapid intuitive "drag and drop" program creation

Only $3,995

ExpressGene™ Gradient Cycler

*Denville Scientific…*Your Source *for* Benchtop Equipment

Pipettes ▪ Centrifuges ▪ Electrophoresis Equipment ▪ Shakers ▪ Rockers www.densci.com DENVILLE SCIENTIFIC INC.

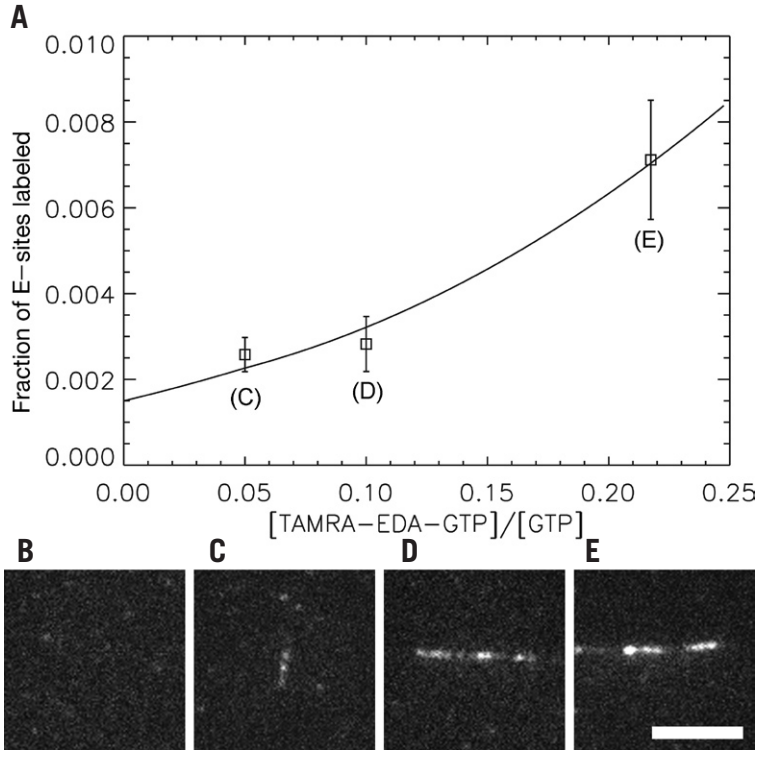

Figure 2. Competition assay between TAMRA-EDA-GTP and unlabeled GTP. (A) Plot of TAMRA-EDA-GTP/GTP occupation (mean ± SEM, $n > 3$) observed in microtubules against solution concentrations of TAMRA-EDA-GTP/GTP during polymerization. Letters correspond to concentrations used in (C–E), line corresponds to fit to equilibrium model (see the Supplementary Materials), indicating GTP binds ~75-fold more tightly than TAMRA-EDA-GTP. (B–E) TIRF microscopy images of microtubules polymerized under conditions in panel A. (B) 1/80 [TAMRA-EDA-GTP]/[GTP], not in panel A due to dimness; (C) 1/20 [TAMRA-EDA-GTP]/[GTP]; (D) 1/10 [TAMRA-EDA-GTP]/[GTP]; (E) 1/5 [TAMRA-EDA-GTP]/[GTP]. Scale bar, 5 µm.

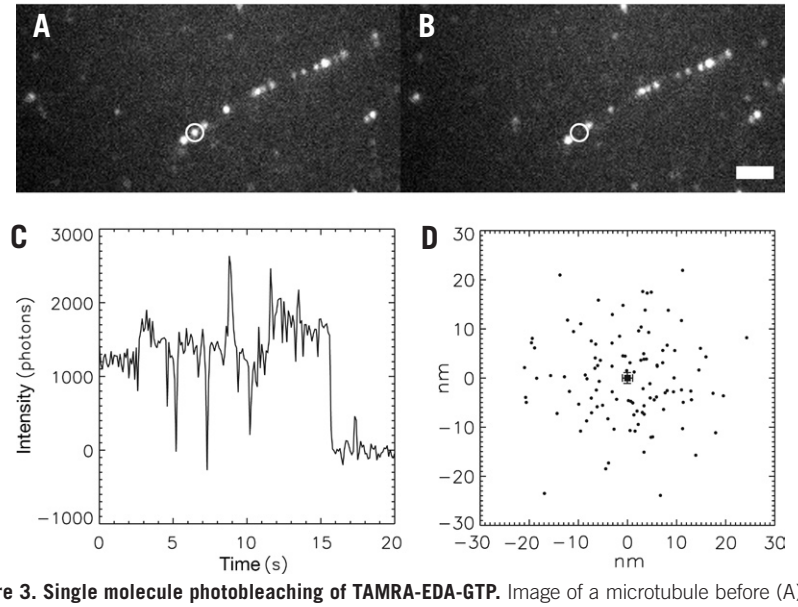

Figure 3. Single molecule photobleaching of TAMRA-EDA-GTP. Image of a microtubule before (A) and after (B) the photobleaching of a single molecule of TAMRA-EDA-GTP (highlighted white circle). Microtubule was polymerized under conditions of Figure 2D. (C) Plot of intensity of highlighted spot versus time collected at 10 Hz. The single sudden drop to 0 photons at about 15 s represents the photobleaching of a single molecule of TAMRA-EDA-GTP. Occasional blinking is evident before irreversible photobleaching. The total integrated intensity in panel C is about 200,000 photons. (D) Plot of positions (•) of the highlighted spot, relative to the mean position. The precision of these positions (standard deviation) is ±9.8 nm. The mean ± SEM (0.93 nm) is shown (■ with error bars). Scale bar, 5 µm.

potential surface binding. Microtubules were separated from free TAMRA-EDA-GTP as described in the Table 1. In this case, microtubules showed no fluorescent labeling. Microtubule presence was confirmed by kinesin-quantum dot labeling, as described in the Materials and methods section. The labeling density of kinesin-quantum dot complexes on TAMRA-EDA-GTP microtubules was similar to the labeling density on unlabeled microtubules ($2.1 \pm 0.5\ \mu m^{-1}$ and $1.2 \pm 0.4\ \mu m^{-1}$, respectively) (Supplementary Figure S1). Furthermore, kinesin-1 motility was examined using a microtubule gliding assay, in which kinesins bound to a glass surface push microtubules through solution (37). At 1 mM (saturating) ATP, microtubules densely labeled with TAMRA-EDA-GTP were pushed by kinesin at 475 ± 20 nm/s (Supplementary Figure S2), similar to previous results. At very low labeling densities (fewer than 1 TAMRA-EDA-GTP/µm), microtubules were pushed by kinesin at 450 ± 15 nm/s (Supplementary Figure S2). Together, the binding and velocity results indicate that TAMRA-EDA-GTP does not interfere with the MAP kinesin-1.

Alternately, TAMRA-EDA-GTP might become incorporated into growing microtubules, albeit not bound at the E-site. To test this possibility, we performed a competition assay between TAMRA-EDA-GTP and unlabeled GTP. If both bind to the E-site, we expect microtubule labeling to increase as the unlabeled GTP concentration decreases. Alternatively, if TAMRA-EDA-GTP binds nonspecifically, we expect microtubule labeling to be constant independent of unlabeled GTP concentration. As Figure 2 shows, we find that decreasing the concentration of unlabeled GTP present during polymerization results in increasing labeling by TAMRA-EDA-GTP. Indeed, the increase exactly follows a model in which both GTP and TAMRA-EDA-GTP bind to the same site at thermodynamic equilibrium, described in the Supplementary Materials. Our model assumes different dissociation constants for GTP and TAMRA-EDA-GTP from tubulin, equilibration of GTP or TAMRA-EDA-GTP on the E-site of unpolymerized tubulin (achieved by premixing GTP and TAMRA-EDA-GTP with tubulin prior to polymerization), and no exchange of nucleotide after polymerization. A fit to this model (solid line in Figure 2) indicates an E-site dissociation constant for TAMRA-EDA-GTP 75-fold weaker than that for GTP. Using literature values for the E-site affinity for GTP (38), we find a dissociation constant of $1.0 \pm 0.4\ \mu M$ for TAMRA-EDA-GTP. In the limit of an infinite concentration of GTP (corresponding to the y-intercept), our model indicates a small residual amount of TAMRA-

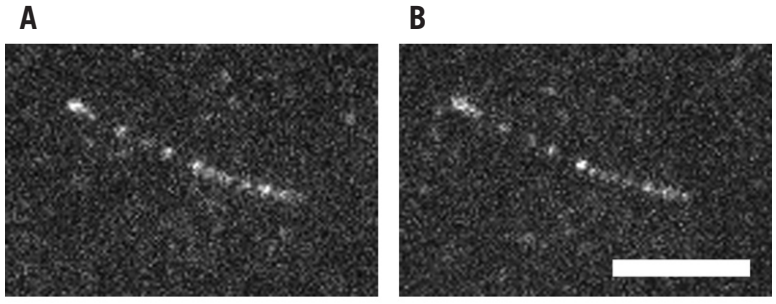

Figure 4. Microtubule labeling is stable for 10 min. Two images of the same microtubule (A) before and (B) after a 10-min interval with no illumination to prevent photobleaching. The pattern of bright spots in the two images is essentially identical, indicating that the positions of molecules of TAMRA-EDA-GTP is stable for at least 10 min. Scale bar, 5 μm.

Table 1. Fluorescent GTP microtubule labeling protocol.

Step	Details
1	Thaw tubulin as quickly and briefly as possible at 37°C. Chill on ice.
2	Spin out insolubles, 20 min at 4°C, ~17,000× *g*.
3	Mix microtubule polymerization solution: tubulin in MT buffer to 5 mg/mL, fluorescent GTP to 20 μM, GTP to 0.2 mM. Solution will be pink for TAMRA and Cy3, blue for Cy5.
4	Incubate for 30 min at 37°C, light-protected (e.g., wrapped in aluminum foil). Solution will turn slightly turbid.
5	Add paclitaxel to 40 μM, mix gently but thoroughly, incubate a further 20 min at 37°C, light-protected.
6	Gently layer MT solution onto a 100-μL, 30% w/v room temperature sucrose cushion. Spin for 20 min at room temperature, ~17,000× *g*. Light gray pellet may or may not be apparent.
7	Draw off colored layer (MT buffer with free fluorescent GTP) from top, leaving clear sucrose cushion.
8	Rinse remaining colored residue with 50 μL 30% (w/v) sucrose buffer, draw off.
9	Draw off clear sucrose cushion, avoiding pellet at bottom of tube.
10	Very gently rinse pellet with 50 μL room temperature storage buffer. Do not resuspend. Draw off buffer.
11	Resuspend pellet in room temperature storage buffer to original volume of step 3 (~5 mg/mL). Store, light-protected, ≤2 weeks, at room temperature.

EDA-GTP labeling: 0.15% ± 0.10% of sites. This residual labeling is much less than the labeling in Figures 1, B–D for comparison. Affinities for Cy3-EDA-GTP and Cy5-EDA-GTP were not determined quantitatively, but Figure 1, B–D shows similar levels of labeling for the three analogs.

To test whether the fluorescent GTP is not only a specific label but also a viable label for single molecule fluorescence, we observed microtubules labeled with TAMRA-EDA-GTP spaced by more than the optical diffraction limit (Figure 3A). We observed that individual fluorescent spots showed single-step photobleaching (Figure 3, B and C), indicating that each spot corresponds to a single TAMRA-EDA-GTP molecule. As the example in Figure 3C shows, a single spot emits $>10^5$ collectable photons. This single spot was also tracked with better than 10 nm precision for 150 frames (Figure 3D), similar to the 5 nm precision expected from single particle tracking theory (39). Indeed, by averaging over all 150 frames, this spot was localized to within 1 nm.

Finally, to ensure that the fluorescent GTP will be useful for a variety of labeling experiments, we tested whether the label remains stably bound to microtubules for long times. If binding is diffusion limited, we expect the micromolar dissociation constant to correspond to a dissociation time constant of about 10–100 s (40). As Figure 4 shows however, the binding is stable for >10 min, indicating TAMRA-EDA-GTP is trapped in the microtubule lattice. In addition, we have observed TAMRA-EDA-GTP microtubules stored for 2 weeks as described in Table 1 (that is, at room temperature, in the dark, and in the absence of free TAMRA-EDA-GTP). These microtubules remain fluorescent, indicating that the TAMRA-EDA-GTP is essentially irreversibly trapped in the microtubule lattice.

In summary, we have shown that a class of fluorescent molecules, GTP modified at the 2′ or 3′ location with a bright organic fluorophore, are a promising label of microtubules. These fluorescent GTP analogs bind to the E-site on tubulin, as indicated by the

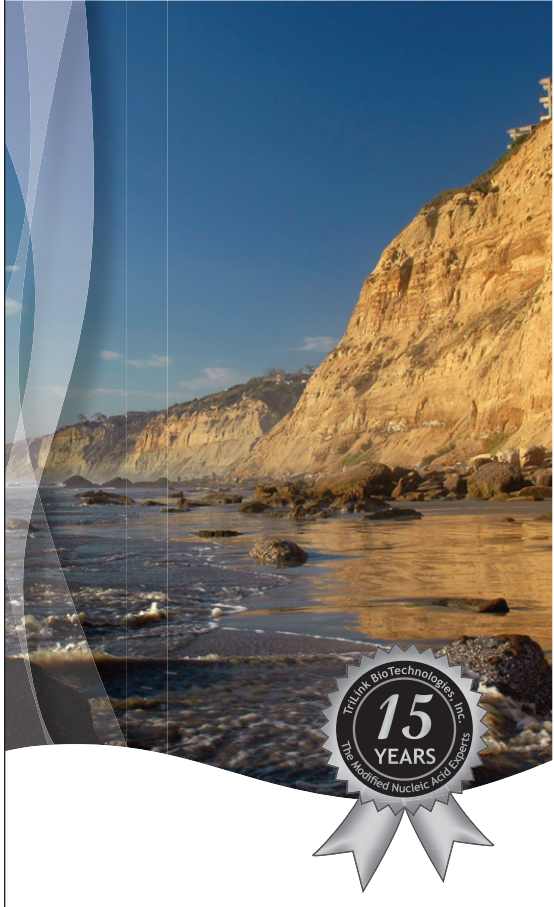

Celebrating 15 Years in Modified Nucleic Acid Synthesis

Specialty Oligonucleotides, Nucleoside Triphosphates and Hot Start PCR Products

Even if you haven't worked directly with TriLink, it is likely that you already use our products. Our nucleic acid products are essential components of many kits and life science tools. Our custom oligonucleotides are key in the Applied Biosystems SOLiD™ System, the Roche NimbleGen DNA microarrays and the GenMark Dx™ eSensor® Detection System. TriLink's CleanAmp™ dNTPs are important reagents in Biofortuna's HLA Diagnostic Kits and ETS Labs' Scorpions™ Wine Spoilage Detection System. Since 1996, our goal has been not only to provide high quality highly-modified nucleic acid solutions, but also to apply our unique expertise to our customers' technical barriers.

TriLink BioTechnologies
The Modified Nucleic Acid Experts
www.trilinkbiotech.com

competition assay of Figure 2, and remain tightly bound for long periods. They do not interfere with the binding of the MAP kinesin-1. We show that they are useable for FIONA measurements when microtubules are sparsely labeled. However, at high microtubule labeling densities (in the absence of unlabeled GTP), we also expect this label to be viable for super-resolution imaging of microtubules via STORM (1). Since Cy3-EDA-GTP labels microtubules well, stochastic switching of E-site bound Cy3-EDA-GTP between bright and dark states would allow protofilament-level resolution of microtubules in an all-optical system, enabling a new class of high-resolution studies of microtubules and the cytoskeleton.

Acknowledgments

This work was supported by the Research Corporation for Science Advancement. We further thank Jeff Gelles and Helen Lee for assistance with the noncommercial version of TAMRA-EDA-GTP.

Competing interests

The authors declare no competing interests.

References

1. **Rust, M.J., M. Bates, and X. Zhuang.** 2006. Sub-diffraction-limit imaging by stochastic optical reconstruction microscopy (STORM). Nat. Methods *3*:793-796.
2. **Betzig, E., G.H. Patterson, R. Sougrat, O.W. Lindwasser, S. Olenych, J.S. Bonifacino, M.W. Davidson, J. Lippincott-Schwartz, and H.F. Hess.** 2006. Imaging intracellular fluorescent proteins at nanometer resolution. Science *313*:1642-1645.
3. **Kural, C., H. Kim, S. Syed, G. Goshima, V.I. Gelfand, and P.R. Selvin.** 2005. Kinesin and dynein move a peroxisome in vivo: a tug-of-war or coordinated movement? Science *308*:1469-1472.
4. **Sako, Y., S. Minoghchi, and T. Yanagida.** 2000. Single-molecule imaging of EGFR signalling on the surface of living cells. Nat. Cell Biol. *2*:168-172.
5. **Yildiz, A., J.N. Forkey, S.A. McKinney, T. Ha, Y.E. Goldman, and P.R. Selvin.** 2003. Myosin V walks hand-over-hand: single fluorophore imaging with 1.5-nm localization. Science *300*:2061-2065.
6. **Lodish, H., A. Berk, P. Matsudaira, C.A. Kaiser, M. Krieger, M.P. Scott, S.L. Zipursky, and J. Darnell.** 2003. Molecular Cell Biology. W.H. Freeman, New York.
7. **Vale, R.D.** 2003. The molecular motor toolbox for intracellular transport. Cell *112*:467-480.
8. **Desai, A. and T.J. Mitchison.** 1997. Microtubule polymerization dynamics. Annu. Rev. Cell Dev. Biol. *13*:83-117.
9. **Amos, L.A. and D. Schlieper.** 2005. Microtubules and MAPs. Adv. Protein Chem. *71*:257-298.
10. **Weber, K., R. Pollack, and T. Bibring.** 1975. Antibody against tubulin: the specific visualization of cytoplasmic microtubules in tissue culture cells. Proc. Natl. Acad. Sci. USA *72*:459-463.
11. **Bre, M.H., R. Pepperkok, A.M. Hill, N. Levilliers, W. Ansorge, E.H.K. Stelzer, and E. Karsenti.** 1990. Regulation of microtubule dynamics and nucleation during polarization in MDCK-II cells. J. Cell Biol. *111*:3013-3021.
12. **Barton, D.A. and R.L. Overall.** 2010. Cryofixation rapidly preserves cytoskeletal arrays of leaf epidermal cells revealing microtubule co-alignments between neighboring cells and adjacent actin and microtubule bundles in the cortex. J. Microsc. *237*:79-88.
13. **Saxton, W.M., D.L. Stemple, R.J. Leslie, E.D. Salmon, M. Zavortink, and J.R. McIntosh.** 1984. Tubulin dynamics in cultured mammalian cells. J. Cell Biol. *99*:2175-2186.
14. **Waterman-Storer, C.M. and E.D. Salmon.** 1997. Actomyosin-based retrograde flow of microtubules in the lamella of migrating epithelial cells influences microtubule dynamic instability and turnover and is associated with microtubule breakage and treadmilling. J. Cell Biol. *139*:417-434.
15. **Chen, W. and D.H. Zhang.** 2004. Kinetochore fibre dynamics outside the context of the spindle during anaphase. Nat. Cell Biol. *6*:227-231.
16. **Van den Heuvel, M.G., M.P. de Graaff, and C. Dekker.** 2008. Microtubule curvatures under perpendicular electric forces reveal a low persistence length. Proc. Natl. Acad. Sci. USA *105*:7941-7946.
17. **Gell, C., V. Bormuth, G.J. Brouhard, D.N. Cohen, S. Diez, C.T. Friel, J. Helenius, B. Nitzsche, et al.** 2010. Microtubule dynamics reconstituted in vitro and imaged by single-molecule fluorescence microscopy. Methods Cell Biol. *95*:221-245.
18. **Evangelio, J.A., M. Abal, I. Barasoain, A.A. Souto, M.P. Lillo, A.U. Acuna, F. Amat-Guerri, and J.M. Andreu.** 1998. Fluorescent taxoids as probes of the microtubule cytoskeleton. Cell Motil. Cytoskeleton *39*:73-90.
19. **Martin, D.S., R. Fathi, T.J. Mitchison, and J. Gelles.** 2010. FRET measurements of kinesin neck orientation reveal a structural basis for processivity and asymmetry. Proc. Natl. Acad. Sci. USA *107*:5453-5458.
20. **Carminati, J.L. and T. Stearns.** 1997. Microtubules orient the mitotic spindle in yeast through dynein-dependent interactions with the cell cortex. J. Cell Biol. *138*:629-641.
21. **Rusan, N.M., C.J. Fagerstrom, A.M.C. Yvon, and P. Wadsworth.** 2001. Cell cycle-dependent changes in microtubule dynamics in living cells expressing green fluorescent protein-alpha tubulin. Mol. Biol. Cell *12*:971-980.
22. **Muraoka, M., H. Fukuzawa, A. Nishida, K. Okano, T. Tsuchihara, A. Shimoda, Y. Suzuki, M. Sato, et al.** 1999. The effects of various GTP analogues on microtubule assembly. Cell Struct. Funct. *24*:101-109.
23. **Yarbrough, L.R. and M. Kirsch.** 1981. Binding of fluorescent analogs of GTP to the exchangeable nucleotide binding site of tubulin. J. Biol. Chem. *256*:112-117.
24. **Muto, E., H. Sakai, and K. Kaseda.** 2005. Long-range cooperative binding of kinesin to a microtubule in the presence of ATP. J. Cell Biol. *168*:691-696.
25. **Diaz, J.F., J.M. Valpuesta, P. Chacon, G. Diakun, and J.M. Andreu.** 1998. Changes in microtubule protofilament number induced by Taxol binding to an easily accessible site. Internal microtubule dynamics. J. Biol. Chem. *273*:33803-33810.
26. **Choi, M.C., U. Raviv, H.P. Miller, M.R. Gaylord, E. Kiris, D. Ventimiglia, D.J. Needleman, M.W. Kim, et al.** 2009. Human microtubule-associated-protein tau regulates the number of protofilaments in microtubules: a synchrotron X-ray scattering study. Biophys. J. *97*:519-527.
27. **Eberth, A., R. Dvorsky, C.F. Becker, A. Beste, R.S. Goody, and M.R. Ahmadian.** 2005. Monitoring the real-time kinetics of the hydrolysis reaction of guanine nucleotide-binding proteins. Biol. Chem. *386*:1105-1114.
28. **Weisenberg, R.C.** 1972. Microtubule formation in vitro in solutions containing low calcium concentrations. Science *177*:1104-1105.
29. **Borisy, G.G., J.M. Marcum, J.B. Olmsted, D.B. Murphy, and K.A. Johnson.** 1975. Purification of tubulin and associated high molecular weight proteins from porcine brain and characterization of microtubule assembly in vitro. Ann. N.Y. Acad. Sci. *253*:107-132.
30. **Friedman, L.J., J. Chung, and J. Gelles.** 2006. Viewing dynamic assembly of molecular complexes by multi-wavelength single-molecule fluorescence. Biophys. J. *91*:1023-1031.
31. **Berliner, E., E.C. Young, K. Anderson, H.K. Mahtani, and J. Gelles.** 1995. Failure of a single-headed kinesin to track parallel to microtubule protofilaments. Nature *373*:718-721.
32. **Young, E.C., H.K. Mahtani, and J. Gelles.** 1998. One-headed kinesin derivatives move by a nonprocessive, low-duty ratio mechanism unlike that of two-headed kinesin. Biochemistry *37*:3467-3479.
33. **Crocker, J.C. and D.G. Grier.** 1996. Methods of digital video microscopy for colloidal studies. J. Colloid Interface Sci. *179*:298-310.
34. **Weisenberg, R.C., G.G. Borisy, and E.W. Taylor.** 1968. The colchicine-binding protein of mammalian brain and its relation to microtubules. Biochemistry *7*:4466-4479.
35. **Mitchison, T.J.** 1993. Localization of an exchangeable GTP binding site at the plus end of microtubules. Science *261*:1044-1047.
36. **Weisenberg, R.C., W.J. Deery, and P.J. Dickinson.** 1976. Tubulin-nucleotide interactions during the polymerization and depolymerization of microtubules. Biochemistry *15*:4248-4254.
37. **Vale, R.D., T.S. Reese, and M.P. Sheetz.** 1985. Identification of a novel force-generating protein, kinesin, involved in microtubule-based motility. Cell *42*:39-50.
38. **Correia, J.J., L.T. Baty, and R.C. Williams, Jr.** 1987. Mg^{2+} dependence of guanine nucleotide binding to tubulin. J. Biol. Chem. *262*:17278-17284.
39. **Thompson, R.E., D.R. Larson, and W.W. Webb.** 2002. Precise nanometer localization analysis for individual fluorescent probes. Biophys. J. *82*:2775-2783.
40. **Berg, O.G. and P.H. von Hippel.** 1985. Diffusion-controlled macromolecular interactions. Annu. Rev. Biophys. Biophys. Chem. *14*:131-160.

Received 14 October 2010; accepted 16 May 2011.

Address correspondence to Douglas S. Martin, Lawrence University, 711 E. Boldt Way, SPC-24, Appleton, WI 54911, USA. e-mail: douglas.s.martin@lawrence.edu

To purchase reprints of this article, contact: biotechniques@fosterprinting.com